

Fairness-Aware Secure Integrated Sensing and Communications with Fractional Programming

Ali Khandan Boroujeni[✉], *Graduate Student Member, IEEE*,

Kuranage Roche Rayan Ranasinghe[✉], *Graduate Student Member, IEEE*,

Giuseppe Thadeu Freitas de Abreu[✉], *Senior Member, IEEE*, Stefan Köpsell[✉], *Senior Member, IEEE*,

Ghazal Bagheri[✉], *Graduate Student Member, IEEE*, and Rafael F. Schaefer[✉], *Senior Member, IEEE*

Abstract—We propose a novel secure integrated sensing and communications (ISAC) system designed to serve multiple communication users (CUs) and targets. To that end, we formulate an optimization problem that maximizes the secrecy rate under constraints balancing both communication and sensing requirements. To enhance fairness among users, an entropy-regularized fairness metric is introduced within the problem framework. We then propose a solution employing an accelerated quadratic transform (QT) with a non-homogeneous bound to iteratively solve two subproblems, thereby effectively optimizing the overall objective. This approach ensures robust security and fairness in resource allocation for ISAC systems. Finally, simulation results verify the performance gains in terms of average secrecy rate, average data rate, and beam gain.

Index Terms—Integrated sensing and communications, Physical-layer security, Beamforming, Optimization, Artificial noise, Fractional programming

I. INTRODUCTION

The evolution of wireless communication systems toward sixth-generation (6G) and beyond has underscored the importance of integrated sensing and communications (ISAC) systems, which unify radar sensing and communication functionalities within a unified spectrum and hardware framework. This convergence addresses the increasing demand for spectral efficiency, cost-effective hardware, and support for emerging applications such as autonomous vehicles, smart cities, augmented reality, and massive Internet-of-things (IoT) deployments [1]–[4]. By enabling simultaneous sensing and communication, ISAC systems offer significant advantages, including enhanced resource utilization, reduced hardware complexity, and improved system scalability [5]–[7]. However, the integration of these dual functionalities introduces multifaceted challenges, including security vulnerabilities, interference management, equitable resource allocation, and computational complexity in multi-user (MU) environments [8]–[11].

Security remains a critical concern in ISAC systems, particularly in scenarios involving malicious targets or eaves-

droppers that threaten both sensing accuracy and communication confidentiality [1], [12]–[14]. The shared spectrum and hardware increase the attack surface, as adversaries could exploit sensing signals to infer sensitive information or disrupt communication links [8], [15]–[17]. To counter these threats, physical layer security (PLS) techniques have gained prominence, leveraging the physical properties of wireless channels to enhance security without relying on conventional cryptographic methods [6], [8], [18]. For example, [2] proposed joint beamforming designs for dual-functional multiple-input multiple-output (MIMO) radar and communication systems to maximize secrecy rates while ensuring reliable sensing performance. Similarly, [12] developed secrecy rate optimization strategies for MIMO communication radar systems, emphasizing the trade-off between security and performance. Other works, such as [5] and [13], have explored robust beamforming techniques to mitigate interference from malicious targets, while [16] and [17] investigated secure waveform designs to enhance PLS in ISAC systems. These studies highlight the need for robust and adaptive strategies to ensure security in adversarial environments.

In MU ISAC systems, ensuring fairness in resource allocation is paramount to preventing performance disparities, particularly when users have diverse quality-of-service (QoS) requirements [9], [10], [19], [20]. Traditional optimization approaches, such as sum-rate maximization [10], [21], [22], often prioritize aggregate system performance, which may favor users with stronger channel conditions, leading to inequitable resource distribution. To address this, fairness-aware frameworks have been proposed, drawing inspiration from resource allocation metrics in shared computer systems [9], [19], [23]. The entropy-based fairness measure introduced by [23] provides a quantitative framework to balance performance between users, which has been adapted for wireless systems [19], [20], [24]. In the context of ISAC, fairness is particularly challenging due to the conflicting objectives of sensing and communication, which compete for limited resources [24]–[27]. Recent studies have proposed fairness-driven beamforming and resource allocation strategies to ensure equitable performance in MU ISAC systems [19], [24], while [28] introduced proportional fairness metrics to balance sensing and communication performance.

The optimization of ISAC systems involves addressing complex, non-convex problems driven by the interplay of sensing, communication, and security constraints [29]–[32].

Ali Khandan Boroujeni, Stefan Köpsell, and Rafael F. Schaefer are with the Barkhausen Institut und Technische Universität Dresden, 01067 Dresden, Germany (emails: ali.khandanboroujeni@barkhauseninstitut.org; {stefan.koepsell,rafael.schaefer}@tu-dresden.de).

Kuranage Roche Rayan Ranasinghe and Giuseppe Thadeu Freitas de Abreu are with the School of Computer Science and Engineering, Constructor University (previously Jacobs University Bremen), Campus Ring 1, 28759 Bremen, Germany (emails: {kranasinghe,gabreu}@constructor.university).

Ghazal Bagheri is with Technische Universität Dresden, 01187 Dresden, Germany (email: ghazal.bagheri@tu-dresden.de).

Fractional programming has emerged as a powerful tool for tackling such problems, offering tractable solutions for power control, beamforming, and scheduling [29], [32]–[34]. The Lagrange dual complex quadratic transform (QT), as explored in [30], provides an efficient framework for decomposing non-convex problems into iterative subproblems, enabling scalable solutions for large-scale systems [31], [34], [35]. This approach has been successfully applied to MIMO radar systems [36]–[39] and secure ISAC designs [5], [6], [13]. Additionally, techniques such as weighted minimum mean squared error (MMSE) optimization [31], alternating direction method of multipliers (ADMM) [40], and successive convex approximation (SCA) [41] have been employed to address the computational complexity of ISAC systems. Recent advances, such as [42] and [43], have proposed hybrid optimization frameworks that combine fractional programming and machine learning to enhance convergence rates and adaptability.

State-of-the-art (SotA) advancements in ISAC systems have focused on improving sensing accuracy, communication reliability, security, and energy efficiency. For instance, [38] proposed joint transmit beamforming for multi-user MIMO communications and radar, achieving enhanced target detection while maintaining communication quality. Similarly, [26] developed dual-functional beamforming strategies that optimize both signal-to-noise ratio (SNR) for communication and Cramér–Rao bound (CRB) for sensing, addressing the inherent trade-offs in ISAC systems [25], [44], [45]. Robust beamforming techniques have been proposed to mitigate interference from malicious targets [6], [13], [16], [46], while [47] introduced adaptive waveform designs to enhance sensing performance in cluttered environments. Machine learning techniques have also gained traction, with [48] proposing deep reinforcement learning for ISAC, [49] developing neural network-based beamforming strategies, and [50] exploring deep learning (DL) for joint sensing and communication. Energy efficiency has been addressed in works such as [51], [52], which proposed energy-efficient designs for ISAC systems to meet the power constraints of practical deployments.

Practical implementation of ISAC systems faces several challenges, including hardware limitations, channel estimation errors, dynamic interference environments, and real-time computational complexity [4], [11], [53]. Accurate channel state information (CSI) is critical for effective beamforming and resource allocation, yet imperfect CSI can significantly degrade performance [54]–[56]. To address this, [53] and [54] proposed robust channel estimation techniques for ISAC systems, while [55] investigated the impact of CSI errors on system performance. Computational complexity remains a significant hurdle, particularly for large-scale systems with multiple users and targets [30], [57]. Low-complexity algorithms, such as those proposed by [57], [58], and [59], aim to reduce computational overhead while maintaining performance. Emerging technologies, such as reconfigurable intelligent surfaces (RIS) [60]–[62] and terahertz (THz) communications [63], [64], offer new opportunities to enhance ISAC performance by improving signal propagation and spectral efficiency. For instance, [61] explored RIS-assisted ISAC systems to enhance coverage and security, while [63] investigated THz bands for high-resolution

sensing and ultra-high-speed communication. Future research directions include the integration of ISAC with edge computing [65], federated learning [66], and quantum communication [67], which will advance the capabilities of ISAC systems.

In this paper, we propose a comprehensive and practical framework for secure multi-user ISAC systems involving multiple communication users (CUs) and multiple targets. This approach builds on prior works in MIMO radar beamforming [36]–[39], secure ISAC designs [5], [6], [13], and fractional programming [29], [32]–[34]. Unlike most existing works that consider only a single target, often under simplified assumptions that limit practical relevance, our formulation accounts for multiple targets, each with the potential to act as an eavesdropper. This introduces new challenges in simultaneously ensuring reliable communication, accurate sensing, and strong protection of confidential information in adversarial environments. We aim to maximize the overall secrecy rate under strict communication and sensing constraints. A key limitation in prior works is the reliance on predefined SINR thresholds for each user, which leads to suboptimal and unfair resource allocation. In particular, beamforming vectors are often optimized just to satisfy these minimum thresholds, favoring users with strong channels while neglecting others. This imbalance compromises fairness and degrades system utility in multi-user scenarios.

To overcome this issue, we introduce an entropy-regularized fairness metric, inspired by Jain’s fairness index (JFI), which provides a continuous and interpretable measure of fairness in resource allocation. JFI is particularly well-suited for wireless communications due to its scale invariance, bounded range, and computational simplicity, making it ideal for multi-objective optimization. Integrating JFI into the beamforming design promotes equitable treatment of users while maintaining strong secrecy performance. To further explore the tradeoff between fairness and throughput, we develop a novel iterative entropy-based tradeoff interpolation scheme that traverses a discretized fairness-throughput spectrum. This procedure enables smooth transitions between fairness-dominated and throughput-dominated regimes, providing deeper insights into system behavior and helping to identify balanced solutions tailored to application needs. We solve the proposed non-convex optimization problem using an efficient Lagrangian dual framework combined with a non-homogeneous complex QT, a novel solution for fractional programming (FP). This approach decomposes the problem into two tractable subproblems, enabling joint optimization of secure beamforming and artificial noise (AN) design. Unlike traditional uses of AN, which focus solely on jamming eavesdroppers, our method also leverages AN to enhance sensing accuracy while aligning it within the null space of legitimate users, thereby avoiding interference with communication signals. Finally, we demonstrate the practical benefits of our approach in large-scale systems, where computational efficiency and scalability are paramount. Our results confirm that the proposed framework is not only secure and fair, but also highly adaptable to emerging wireless technologies such as 6G ISAC networks.

The remainder of this paper is organized as follows. Section II presents the system model and problem formulation, includ-

ing the proposed metrics to be optimized. Section III details the full formulation of the optimization problem. Section IV presents the solution methodology based on the Lagrange dual complex QT. Section V provides simulation results and performance analysis to validate the proposed approach, and Section VI concludes the paper with future research directions.

The contributions of this paper are summarized as follows:

- We formulate a secure MU-ISAC system that considers multiple targets as potential eavesdroppers, capturing realistic adversarial settings.
- A fairness-aware beamforming design is proposed by integrating an entropy-regularized Jain's index, overcoming the limitations of fixed SINR thresholds.
- An iterative tradeoff scheme is introduced to smoothly navigate the fairness-throughput spectrum, enabling flexible system tuning.
- The non-convex problem is efficiently solved using a dual fractional programming approach that employs a non-homogeneous QT, enabling closed-form updates that avoid costly matrix inversions and accelerate convergence.
- AN is jointly optimized to enhance both secrecy and sensing, while being confined to the null space of communication users to prevent interference.
- The overall framework is scalable and well-suited for large-scale MIMO ISAC deployments in next-generation wireless networks.

II. SYSTEM MODEL

Consider a MU environment with a single BS employing countermeasures against potential eavesdroppers, hereafter referred to as Eves, which are represented by radar targets, while serving CUs. As depicted in Fig. 1, the BS is equipped with N_t transmit antennas, enabling the use of multi-antenna signal processing techniques, such as beamforming and AN

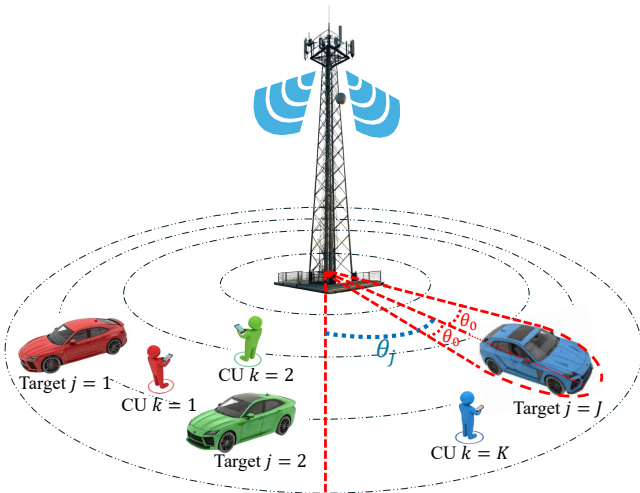


Fig. 1. System model of a secure MU-ISAC network, where a multi-antenna BS serves K CUs while sensing J targets that may act as eavesdroppers. Each target's direction θ_j is assumed to be pre-estimated.

injection, to both enhance communication performance and enable security features.

In this scenario, the BS serves as the central node for managing communication with K CUs, while localizing J radar targets (Eves), and ensuring secure information transmission by mitigating eavesdropping threats from the aforementioned targets. The K legitimate CUs, each with a single receive antenna, are the intended recipients of the transmitted signals and leverage the spatial diversity and secure transmission strategies implemented by the BS to enhance their communication performance. The network also considers that the J untrusted targets are equipped with eavesdropping capabilities. The location of each radar target is assumed to be pre-estimated, with θ_j denoting the direction of the j -th target. Ensuring secure communication against potential eavesdroppers is a critical aspect of system design, which we carefully address in the upcoming sections.

A. Transmit Signal Model

Leveraging both transmit beamforming and AN, the effective transmit signal can be defined as

$$\mathbf{x} = \mathbf{W}\mathbf{s} + \mathbf{n}_{\text{eff}} \in \mathbb{C}^{N_t \times 1}, \quad (1)$$

where $\mathbf{s} \triangleq [s_1, \dots, s_k, \dots, s_K]^T \in \mathbb{C}^{K \times 1}$ represents the symbol vector containing data intended for the K legitimate users. Here, s_k represents the input data symbols drawn from a phase shift keying (PSK) constellation, where the uniform amplitude simplifies symbol normalization and enhances secrecy rate optimization. The beamforming matrix $\mathbf{W} = [\mathbf{w}_1, \dots, \mathbf{w}_k, \dots, \mathbf{w}_K] \in \mathbb{C}^{N_t \times K}$, with $\mathbf{w}_k \in \mathbb{C}^{N_t \times 1}$ denoting the beamforming vector of the k -th user, is designed to optimize the secrecy rate for the intended CUs while reducing the risk of interception by potential eavesdroppers. Notably, \mathbf{W} exploits the spatial diversity provided by the N_t antennas of the base station (BS). The term $\mathbf{n}_{\text{eff}} \in \mathbb{C}^{N_t \times 1} \sim \mathcal{CN}(0, \mathbf{R}_{\text{n}_{\text{eff}}})$ denotes the effective artificial noise (AN) vector with covariance matrix $\mathbf{R}_{\text{n}_{\text{eff}}}$, which is intentionally injected to degrade the interception capabilities of untrusted targets, enhance sensing performance, and create minimal interference to legitimate CUs while inducing significant disruption at potential eavesdroppers.

The primary objective of the system is to achieve secure and reliable communication for the K legitimate CUs while ensuring that the information leakage to the J untrusted targets is minimized. This is accomplished through the joint design of the beamforming matrix \mathbf{W} and the effective AN \mathbf{n}_{eff} , leveraging the multiple antennas at the BS and the advanced optimization techniques.

B. Received Signal Model

Assuming that CUs can be treated as radar targets, and defining $Q \triangleq K + J$, the reflected echoes from these targets at the BS can be expressed as

$$\begin{aligned} \mathbf{r} &= \sum_{q=1}^Q \underbrace{\alpha_q^2 \mathbf{a}(\theta_q)^T \mathbf{a}(\theta_q)}_{\mathbf{G} \in \mathbb{C}^{N_t \times N_t}} \mathbf{x} + \mathbf{z} \\ &= \mathbf{G}(\mathbf{W}\mathbf{s} + \mathbf{n}_{\text{eff}}) + \mathbf{z}. \end{aligned} \quad (2)$$

Let α_q denote the complex path gain from the transmitter to the potential target q . The transmit array steering vector $\mathbf{a}(\theta_q) \in \mathbb{C}^{N_t \times 1}$, corresponding to an arbitrary spatial direction θ_q in the far field, is given by

$$\mathbf{a}(\theta_q) = \left[1, e^{j2\pi \frac{d_M}{\lambda} \sin(\theta_q)}, \dots, e^{j2\pi \frac{d_M}{\lambda} (N_t-1) \sin(\theta_q)} \right]^T, \quad (3)$$

where d_M represents the inter-element spacing of the transmit array (in meters), and λ is the signal wavelength. The background additive white Gaussian noise (AWGN) at the BS is modeled as $\mathbf{z} \sim \mathcal{CN}(0, \sigma_r^2 \mathbf{I})$, where σ_r^2 denotes the background noise power.

C. Performance Metrics

This paper aims to maximize the *sum secrecy rate* of a MU ISAC system in the presence of multiple potential eavesdropping targets. The secrecy rate of each legitimate user is defined as the difference between the achievable rate at the intended receiver and the maximum rate achievable by any eavesdropper, ensuring secure communication at the physical layer. Hence, the secrecy rate for the k -th user is given by

$$\text{SR}_k = \left[\log_2(1 + \rho_k^L) - \max_j (\log_2(1 + \rho_{k,j}^E)) \right]^+, \quad (4)$$

where ρ_k^L denotes the signal to interference-plus-noise ratio (SINR) ratio at the k -th legitimate user, and $\rho_{k,j}^E$ represents the signal-to-noise ratio of the k -th user's signal as intercepted by the j -th eavesdropper. The operator $[\cdot]^+$ ensures that the secrecy rate remains non-negative.

The SINR at the k -th legitimate user is defined as [1]

$$\begin{aligned} \rho_k^L &= \frac{\mathbb{E} \left[|\mathbf{h}_k \mathbf{w}_k s_k|^2 \right]}{\sum_{i \neq k} \mathbb{E} \left[|\mathbf{h}_k \mathbf{w}_i s_i|^2 \right] + \mathbb{E} \left[|\mathbf{h}_k \mathbf{n}_{\text{eff}}|^2 \right] + \sigma_{z_k}^2} \\ &= \frac{\mathbf{h}_k \mathbf{W}_k \mathbf{h}_k^H \|\mathbf{s}_k\|^2}{\sum_{i \neq k} \mathbf{h}_k \mathbf{W}_i \mathbf{h}_k^H \|\mathbf{s}_i\|^2 + \mathbf{h}_k \mathbf{R}_{\text{eff}} \mathbf{h}_k^H + \sigma_{z_k}^2}, \end{aligned} \quad (5)$$

where $\mathbf{h}_k \in \mathbb{C}^{1 \times N_t}$ represents the channel vector from the transmitter to the k -th CU, $\mathbf{W}_k = \mathbf{w}_k \mathbf{w}_k^H$ denotes the beamforming covariance matrix of a given user k , and $\mathbf{R}_{\text{eff}} \in \mathbb{C}^{N_t \times N_t}$ is the covariance matrix of the effective AN. Moreover, the term $\sigma_{z_k}^2$ represents the variance of the AWGN at the k -th legitimate user's receiver. Considering PSK-modulated symbols, we have $\|\mathbf{s}_k\|^2 = 1$.

The received SNR at the j -th eavesdropping target, resulting from the k -th legitimate user's signal, is expressed as

$$\rho_{k,j}^E = \frac{|\alpha_j|^2 \mathbf{a}^H(\theta_j) \mathbf{W}_k \mathbf{a}(\theta_j)}{|\alpha_j|^2 \mathbf{a}^H(\theta_j) \mathbf{R}_{\text{eff}} \mathbf{a}(\theta_j) + \sigma_e^2}, \quad (6)$$

where α_j is the complex path gain from the transmitter to eavesdropper E_j , and $\mathbf{a}(\theta_j)$ is the array steering vector in the direction of eavesdropper j .

Based on the above definitions, the total system secrecy rate can be defined as

$$\text{SR} \triangleq \sum_{k=1}^K \left[\log_2(1 + \rho_k^L) - \max_j (\log_2(1 + \rho_{k,j}^E)) \right]^+. \quad (7)$$

This objective function seeks to optimize the overall confidentiality of the system by enhancing the SINR at legitimate users while minimizing the potential SNR leakage to any of the eavesdroppers. The worst-case eavesdropping scenario is considered via the max operator, thereby ensuring robustness in secure communication design.

III. OPTIMIZATION FORMULATION AND FAIRNESS-AWARE STRATEGY

One of the key contributions of this work is the careful and strategic design of constraints for the proposed ISAC system. Instead of relying on conventional formulations, we introduce a novel set of constraints that align with the system's unique objectives and secrecy performance optimization. These constraints ensure that the intentional generation of AN reinforces radar detection capabilities while avoiding interference with authorized CUs for maintaining communications quality. Additionally, power limitations and QoS requirements are incorporated to guarantee system feasibility and to maximize the overall secrecy rate.

A. Constraints on Communications Performance

To prevent interference with the legitimate communication users, the AN vector \mathbf{n}_{eff} is designed to lie in the null space of the communication users' channel matrix. Let $\mathbf{H} = [\mathbf{h}_1^T, \dots, \mathbf{h}_K^T]^T \in \mathbb{C}^{K \times N_t}$ be the concatenated channel matrix of all communication users. Then, the projected effective noise can be defined as

$$\mathbf{n}_{\text{eff}} = \mathbf{P}^\perp \mathbf{n}, \quad (8)$$

where \mathbf{P}^\perp is the orthogonal projection matrix onto the null space of \mathbf{H} , which can be calculated as

$$\mathbf{P}^\perp = \mathbf{I}_{N_t} - \mathbf{H}^H (\mathbf{H} \mathbf{H}^H)^{-1} \mathbf{H}, \quad (9)$$

with \mathbf{n} denoting the AN vector to be optimized. Consequently, the covariance of the effective AN becomes

$$\mathbf{R}_{\text{eff}} = \mathbf{P}^\perp \mathbf{R}_n (\mathbf{P}^\perp)^H, \quad (10)$$

where $\mathbf{R}_n \triangleq \mathbb{E}[\mathbf{n} \mathbf{n}^H]$. This guarantees that AN does not interfere with the desired communication signals.

On the other hand, many existing works (e.g., [1], [12]) introduce the following constraint to ensure that the SINR at each k -th legitimate user meets a minimum threshold γ_k , thereby guaranteeing the required communication QoS for all users.

$$\rho_k^L \geq \gamma_k, \quad \forall k. \quad (11)$$

However, such predefined SINR thresholds often lead to suboptimal and unfair resource allocation, as the beamforming vectors are typically optimized just to meet the minimum requirements, favoring users with stronger channels while marginalizing those with weaker links. This imbalance undermines fairness and reduces overall system utility in multi-user scenarios. To address this issue, we replace the fixed SINR constraints with JFI in III-C, a simple, interpretable, and normalized metric that effectively promotes equitable resource distribution, making it particularly suitable for multi-user wireless systems [23].

B. Constraints on Sensing Performance

To ensure the sensing functionality is preserved, the received power at each radar target must exceed a predefined threshold η_j . Let $\mathbf{a}(\theta_j)$ denote the steering vector corresponding to direction θ_j , with the same structure as in equation (3). The received radar power at the j -th target is

$$P_j = \alpha_j \mathbf{a}^H(\theta_j) \underbrace{\left(\sum_{k=1}^K \mathbf{w}_k \mathbf{w}_k^H + \mathbf{R}_{n_{\text{eff}}} \right)}_{\tilde{\mathbf{W}}} \mathbf{a}(\theta_j). \quad (12)$$

Thus, the radar power constraint at each target j becomes

$$\mathbf{a}^H(\theta_j) \tilde{\mathbf{W}} \mathbf{a}(\theta_j) \alpha_j \geq \eta_j. \quad (13)$$

Motivated by the 3 dB main-beamwidth design for MIMO radar in [68], we propose a method that constrains the main-beam width within a specified angular interval θ_0 , where θ_0 is a pre-defined angle such that $2\theta_0$ is equal to the desired 3-dB beam width of the waveform, given by

$$\mathbf{a}^H(\theta_j \pm \theta_0) \tilde{\mathbf{W}} \mathbf{a}(\theta_j \pm \theta_0) \alpha_j \leq \frac{\eta_j}{2}, \quad \forall j, \quad (14)$$

where this constraint enforces a main beamwidth of $2\theta_0$, ensuring sufficient angular resolution for reliable radar target detection.

C. Final Optimization Problem

Considering the design variables and constraints, the complete joint optimization problem can be formulated as

$$\begin{aligned} \max_{\mathbf{w}_k, \mathbf{n}} \text{SR} = & \sum_{k=1}^K \left[\log_2 \left(1 + \frac{\mathbf{h}_k \mathbf{w}_k \mathbf{w}_k^H \mathbf{h}_k^H}{\sum_{i \neq k} \mathbf{h}_k \mathbf{w}_i \mathbf{w}_i^H \mathbf{h}_k^H + \mathbf{h}_k \mathbf{n}_{\text{eff}} \mathbf{n}_{\text{eff}}^H \mathbf{h}_k^H + \sigma_k^2} \right) \right. \\ & \left. - \max_j \log_2 \left(1 + \frac{\alpha_j^2 \mathbf{a}^H(\theta_j) \mathbf{w}_k \mathbf{w}_k^H \mathbf{a}(\theta_j)}{\alpha_j^2 \mathbf{a}^H(\theta_j) \mathbf{n}_{\text{eff}} \mathbf{n}_{\text{eff}}^H \mathbf{a}(\theta_j) + \sigma_e^2} \right) \right]^+ \end{aligned}$$

subject to

$$\begin{aligned} \text{(a)} \quad & \text{Tr}(\mathbf{w}_k \mathbf{w}_k^H) \leq P_k, \quad \forall k, \\ \text{(b)} \quad & \text{Tr}(\mathbf{R}_{n_{\text{eff}}}) + \sum_{k=1}^K P_k \leq P_A, \\ \text{(c)} \quad & \rho_k^L \geq \gamma_k, \quad \forall k, \\ \text{(d)} \quad & \mathbf{a}^H(\theta_j) \tilde{\mathbf{W}} \mathbf{a}(\theta_j) \alpha_j \geq \eta_j, \quad \forall j, \\ \text{(e)} \quad & \mathbf{a}^H(\theta_j \pm \theta_0) \tilde{\mathbf{W}} \mathbf{a}(\theta_j \pm \theta_0) \alpha_j \leq \frac{\eta_j}{2}, \quad \forall j. \end{aligned} \quad (15)$$

This formulation ensures that the AN is optimally projected to prevent interference with the communication functionality, while the sensing performance is preserved through power guarantees in desired directions, with the leakage to undesired directions controlled and the total transmit power remaining within system limits.

To address the non-smoothness and non-convexity introduced by the $[\cdot]^+$ operator and the \max_j term in the original secrecy rate expression, we reformulate the problem by maximizing a weighted sum-rate of legitimate users subject to secrecy constraints that upper-bound the eavesdroppers' achievable rates.

This transformation converts the original intractable objective into a smooth and more tractable form, enabling the use of standard optimization techniques while ensuring a predefined level of secrecy. The equivalent problem can then be cast as

$$\max_{\mathbf{w}_k, \mathbf{n}_{\text{eff}}} \sum_{k=1}^K \mu_k \log_2 \left(1 + \frac{\mathbf{h}_k \mathbf{w}_k \mathbf{w}_k^H \mathbf{h}_k^H}{\sum_{i \neq k} \mathbf{h}_k \mathbf{w}_i \mathbf{w}_i^H \mathbf{h}_k^H + \mathbf{h}_k \mathbf{n}_{\text{eff}} \mathbf{n}_{\text{eff}}^H \mathbf{h}_k^H + \sigma_k^2} \right)$$

subject to:

$$\begin{aligned} \text{(a)} \quad & \log_2 \left(1 + \frac{\alpha_j^2 \mathbf{a}^H(\theta_j) \mathbf{w}_k \mathbf{w}_k^H \mathbf{a}(\theta_j)}{\alpha_j^2 \mathbf{a}^H(\theta_j) \mathbf{n}_{\text{eff}} \mathbf{n}_{\text{eff}}^H \mathbf{a}(\theta_j) + \sigma_e^2} \right) \leq \beta_j, \quad \forall j \\ \text{(b)} \quad & \text{Tr}(\mathbf{w}_k \mathbf{w}_k^H) \leq P_k, \quad \forall k, \\ \text{(c)} \quad & \text{Tr}(\mathbf{R}_{n_{\text{eff}}}) + \sum_{k=1}^K P_k \leq P_A, \\ \text{(d)} \quad & \mathbf{a}^H(\theta_j) \tilde{\mathbf{W}} \mathbf{a}(\theta_j) \alpha_j \geq \eta_j, \quad \forall j, \\ \text{(e)} \quad & \mathbf{a}^H(\theta_j \pm \theta_0) \tilde{\mathbf{W}} \mathbf{a}(\theta_j \pm \theta_0) \alpha_j \leq \frac{\eta_j}{2}, \quad \forall j, \end{aligned} \quad (16)$$

which can be iteratively divided into two optimization sub-problems, one for optimizing over \mathbf{w}_k and the other for optimizing over \mathbf{n} .

To circumvent the non-convexity of constraint (c) in (15), we reformulate the original problem by introducing a fairness-aware metric based on Jain's index, defined as

$$F_{\text{SINR}}(\boldsymbol{\mu}) \triangleq \frac{\left[\sum_{k=1}^K \mu_k \cdot \rho_k^L \right]^2}{K \sum_{k=1}^K (\mu_k \cdot \rho_k^L)^2}. \quad (17)$$

This index satisfies $\frac{1}{K} \leq F_{\text{SINR}}(\boldsymbol{\mu}) \leq 1$, where equality with 1 holds if and only if the SINRs are equal across users, i.e., perfectly fair allocation. To guarantee a minimum level of fairness, we impose the constraint $F_{\text{SINR}}(\boldsymbol{\mu}) \geq \xi_F$, where $\xi_F \in (\frac{1}{K}, 1]$ is a design threshold. We seek to determine the weight vector $\boldsymbol{\mu} \in \mathbb{R}_+^K$ lying on the probability simplex $\Delta = \{\boldsymbol{\mu} \in \mathbb{R}_+^K : \sum_{k=1}^K \mu_k = 1\}$, which balances throughput and fairness based on a trade-off parameter $\chi \in [0, 1]$. The composite optimization objective is expressed as

$$\max_{\boldsymbol{\mu} \in \Delta} (1 - \chi) G \sum_{k=1}^K \mu_k \log_2(1 + \rho_k^L) + \chi F_{\text{SINR}}(\boldsymbol{\mu}), \quad (18)$$

where G is a normalization constant defined to ensure that both terms in (18) are normalized to the unit interval, i.e.,

$$G \triangleq \left(\max_{\boldsymbol{\mu} \in \Delta} \sum_{k=1}^K \mu_k \log_2(1 + \rho_k^L) \right)^{-1}. \quad (19)$$

D. Closed-Form Solutions at Extreme Tradeoff Values

We can identify two analytically tractable edge cases to obtain closed-form solutions.

- *Throughput Maximization* ($\chi = 0$): The objective function reduces to a weighted sum-rate maximization, where the optimal solution places all the weight on the user with the highest SINR (in the absence of regularization).

- *Fairness Maximization* ($\chi = 1$): The fairness metric F_{SINR} is maximized when the effective SINRs are equalized, leading to the solution

$$\mu_k^* = \frac{c}{\rho_k^L}, \quad \text{where } c = \left(\sum_{k=1}^K \frac{1}{\rho_k^L} \right)^{-1}. \quad (20)$$

E. Entropy-Regularized Iterative Optimization Strategy

To interpolate between the extreme regimes of fairness and throughput, we propose an iterative procedure over a discretized tradeoff path $\{\chi_t\}_{t=0}^T$, transitioning from full fairness ($\chi_0 = 1$) to full throughput ($\chi_T = 0$). To ensure stability and explore smoother solutions, we incorporate entropy regularization into the objective as

$$\begin{aligned} \mathcal{L}(\boldsymbol{\mu}; \chi_t) = & (1 - \chi_t)G \sum_{k=1}^K \mu_k \log_2(1 + \rho_k^L) \\ & + \chi_t F_{\text{SINR}}(\boldsymbol{\mu}) - \nu H(\boldsymbol{\mu}), \end{aligned} \quad (21)$$

where $H(\boldsymbol{\mu}) = -\sum_{k=1}^K \mu_k \log \mu_k$ denotes the Shannon entropy and $\nu > 0$ is a regularization parameter that encourages diversity in the weight allocation. The parameter ν is selected to balance smoothness and concentration. Typical values are empirically chosen to maintain solution sparsity while avoiding degeneracy.

The gradient of \mathcal{L} with respect to μ_k is given by

$$\begin{aligned} \nabla_{\mu_k} \mathcal{L} = & (1 - \chi_t)G \log_2(1 + \rho_k^L) \\ & + \chi_t \left[\frac{2(\boldsymbol{\mu}^T \mathbf{r})r_k}{K \|\boldsymbol{\mu} \circ \mathbf{r}\|^2} - \frac{2(\boldsymbol{\mu}^T \mathbf{r})^2 r_k^2}{K \|\boldsymbol{\mu} \circ \mathbf{r}\|^4} \right] - \nu(1 + \log \mu_k), \end{aligned} \quad (22)$$

where $\mathbf{r} = [\rho_1^L, \dots, \rho_K^L]^T$, and \circ denotes element-wise multiplication.

Algorithm 1 Enhanced H-FRO: Hybrid Fairness–Rate Optimization with Fairness Penalty and Entropy Regularization

- 1: **Input:** Initial weights $\mu_k^{(0)} = \frac{1}{K}$, tradeoff path $\{\chi_t\}_{t=0}^T$, minimum fairness ξ_F , entropy weight $\nu > 0$, penalty weight $\lambda > 0$, trust region rate $\eta \in (0, 1]$, inner iterations I
- 2: **Output:** Optimized weight vector $\boldsymbol{\mu}^{(T)}$ and final sum secrecy rate
- 3: Calculate SINR vector $\boldsymbol{\rho}^L$ via Algorithm 2.
- 4: Define simplex $\Delta := \{\boldsymbol{\mu} \in \mathbb{R}_+^K : \sum_k \mu_k = 1\}$.
- 5: Initialize $\mu_k^{(1)} \leftarrow \frac{1/\rho_k^L}{\sum_{k=1}^K 1/\rho_k^L}$, $\forall k$.
- 6: **for** $t = 1$ to T **do**
- 7: Set $\chi \leftarrow \chi_t$, $\boldsymbol{\mu} \leftarrow \boldsymbol{\mu}^{(t-1)}$, $\boldsymbol{\mu}_{\text{old}} \leftarrow \boldsymbol{\mu}$.
- 8: **for** $i = 1$ to I **do**
- 9: Compute gradient $\nabla_{\mu_k} \mathcal{L}_{\text{penalized}}$ via (22).
- 10: Update $\boldsymbol{\mu} \leftarrow \boldsymbol{\mu} + \alpha \cdot \nabla_{\boldsymbol{\mu}}$.
- 11: Project $\boldsymbol{\mu}$ onto simplex Δ .
- 12: Apply trust region: $\boldsymbol{\mu} \leftarrow (1 - \eta)\boldsymbol{\mu}_{\text{old}} + \eta\boldsymbol{\mu}$.
- 13: **end for**
- 14: Set $\boldsymbol{\mu}^{(t)} \leftarrow \boldsymbol{\mu}$.
- 15: **end for**
- 16: **Return:** $\boldsymbol{\mu}^{(T)}$
- 17: Update secrecy rate using Algorithm 2 with optimal $\boldsymbol{\mu}^{(T)}$

To address the non-convex fairness constraint, we adopt a *penalty-based relaxation* rather than hard projection. Specifically, the fairness constraint $F_{\text{SINR}} \geq \xi_F$ is encoded into the objective via a differentiable penalty defined by

$$\mathcal{L}_{\text{penalized}}(\boldsymbol{\mu}; \chi_t) \triangleq \mathcal{L}(\boldsymbol{\mu}; \chi_t) - \lambda \cdot (\max(0, \xi_F - F_{\text{SINR}}(\boldsymbol{\mu})))^2, \quad (23)$$

where $\lambda > 0$ is a penalty coefficient controlling constraint enforcement. This approach avoids projection onto a non-convex set and ensures differentiability.

The proposed approach integrates multiple convex components (entropy, throughput) with a non-convex fairness penalty, yielding a *partially non-convex* landscape and is summarized in Algorithm 1. While global optimality is not guaranteed, the use of entropy regularization and gradual transition over $\{\chi_t\}$ promotes smooth convergence to locally optimal and practically fair solutions.

IV. DUAL OPTIMIZATION FRAMEWORK

In this section, we develop a dual optimization framework to tackle the joint beamforming and noise design problem by decomposing it into two subproblems. The first subproblem optimizes the beamforming vectors assuming fixed noise, reformulating the original non-convex problem into a more tractable form via auxiliary variables and a dual QT. This approach enables closed-form updates for key variables and leverages convex constraints to efficiently solve the problem. Subsequent subsections detail the problem formulation, the dual QT application, and the derivation of optimal solutions for the introduced auxiliary variables.

A. Subproblem I: Non-homogeneous QT for Beamforming

Let us first consider the optimization over \mathbf{w}_k , under the assumption that \mathbf{n} is fixed. In addition, in order to make the optimization more tractable, we allocate the constraints (a) and (b) from (16) to the first subproblem and the constraints (c-e) to the second subproblem. Then, the equivalent first optimization problem can be expressed as

$$\begin{aligned} \max_{\mathbf{w}_k} \quad & \sum_{k=1}^K \mu_k \log_2(1 + M_k(\mathbf{w}_k)) \\ \text{subject to:} \quad & \\ & \text{(a) } \log_2 \left(1 + \frac{\alpha_j^2 \mathbf{a}^H(\theta_j) \mathbf{w}_k \mathbf{w}_k^H \mathbf{a}(\theta_j)}{\alpha_j^2 \mathbf{a}^H(\theta_j) \mathbf{n}_{\text{eff}} \mathbf{n}_{\text{eff}}^H \mathbf{a}(\theta_j) + \sigma_e^2} \right) \leq \beta_j, \quad \forall j, \\ & \text{(b) } \text{Tr}(\mathbf{w}_k \mathbf{w}_k^H) \leq P_k, \quad \forall k, \end{aligned} \quad (24)$$

where we use the definition

$$M_k(\mathbf{w}_k) \triangleq e_k^*(\mathbf{w}_k) B_k^{-1}(\mathbf{w}_k) e_k(\mathbf{w}_k), \quad (25)$$

where $(\cdot)^*$ is the complex conjugate with $e_k(\mathbf{w}_k) \triangleq \mathbf{h}_k \mathbf{w}_k \in \mathbb{C}$ and $B_k(\mathbf{w}_k) \in \mathbb{C}$ denoting a covariance value that captures the interference from other users and noise effects given by

$$B_k(\mathbf{w}_k) = \sum_{i \neq k} \mathbf{h}_k \mathbf{w}_i \mathbf{w}_i^H \mathbf{h}_k^H + \mathbf{h}_k \mathbf{n}_{\text{eff}} \mathbf{n}_{\text{eff}}^H \mathbf{h}_k^H + \sigma_k^2. \quad (26)$$

Let us first note that the constraint (a) in equation (24) can be expressed as a convex inequality if \mathbf{n} is held fixed. Therefore, the constraint

$$\log_2 \left(1 + \frac{\alpha_j^2 \mathbf{a}^H(\theta_j) \mathbf{w}_k \mathbf{w}_k^H \mathbf{a}(\theta_j)}{\alpha_j^2 \mathbf{a}^H(\theta_j) \mathbf{n}_{\text{eff}}^H \mathbf{n}_{\text{eff}}^H \mathbf{a}(\theta_j) + \sigma_e^2} \right) \leq \beta_j, \quad (27)$$

can be equivalently expressed as

$$\mathbf{w}_k^H \mathbf{a}(\theta_j) \mathbf{a}^H(\theta_j) \mathbf{w}_k \leq \frac{(\alpha_j^2 - 1)(\alpha_j^2 \mathbf{a}^H(\theta_j) \mathbf{n}_{\text{eff}}^H \mathbf{n}_{\text{eff}}^H \mathbf{a}(\theta_j) + \sigma_e^2)}{\alpha_j^2}. \quad (28)$$

Leveraging the above, the main sub-optimization portrayed in equation (24) can be reformulated as follows [29], [33].

$$h(\mathbf{w}_k, \boldsymbol{\zeta}) = \sum_{k=1}^K \mu_k \left[\log_2(1 + \zeta_k) - \zeta_k + (1 + \zeta_k) e_k^*(\mathbf{w}_k) (e_k(\mathbf{w}_k) e_k^*(\mathbf{w}_k) + B_k(\mathbf{w}_k))^{-1} e_k(\mathbf{w}_k) \right], \quad (29)$$

where $\boldsymbol{\zeta} \triangleq \{\zeta_1, \dots, \zeta_K\}$ denotes a set of auxiliary variables.

Let us now also define $\hat{B}_k(\mathbf{w}_k) \triangleq e_k(\mathbf{w}_k) e_k^*(\mathbf{w}_k) + B_k(\mathbf{w}_k)$ and $\hat{M}_k(\mathbf{w}_k) \triangleq e_k^*(\mathbf{w}_k) \hat{B}_k^{-1}(\mathbf{w}_k) e_k(\mathbf{w}_k)$.

Leveraging the above definitions, the optimization problem defined in equation (24) can be reformulated as

$$\begin{aligned} \max_{\mathbf{w}_k, \boldsymbol{\zeta}} h(\mathbf{w}_k, \boldsymbol{\zeta}) &= \sum_{k=1}^K \mu_k \left[(1 + \zeta_k) \hat{M}_k(\mathbf{w}_k) + \log_2(1 + \zeta_k) - \zeta_k \right] \\ \text{subject to:} \\ (a) \quad &\log_2 \left(1 + \frac{\alpha_j^2 \mathbf{a}^H(\theta_j) \mathbf{w}_k \mathbf{w}_k^H \mathbf{a}(\theta_j)}{\alpha_j^2 \mathbf{a}^H(\theta_j) \mathbf{n}_{\text{eff}}^H \mathbf{n}_{\text{eff}}^H \mathbf{a}(\theta_j) + \sigma_e^2} \right) \leq \beta_j, \quad \forall j, \\ (b) \quad &\text{Tr}(\mathbf{w}_k \mathbf{w}_k^H) \leq P_k, \quad \forall k. \end{aligned} \quad (30)$$

Next, by utilizing a dual complex QT, we can re-express $\hat{M}_k(\mathbf{w}_k)$ as

$$\hat{M}_k(\mathbf{w}_k) = 2\text{Re}\{y_k^* e_k(\mathbf{w}_k)\} - y_k^* \hat{B}_k(\mathbf{w}_k) y_k, \quad (31)$$

where $y_k \in \mathbb{C}$ is an auxiliary variable.

Substituting the definition of $\hat{B}_k(\mathbf{w}_k)$ into the second term of equation (31), one can further evaluate that

$$\begin{aligned} y_k^* \hat{B}_k(\mathbf{w}_k) y_k &= \mathbf{w}_k^H \left(\mathbf{h}_k^H y_k y_k^* \mathbf{h}_k + \sum_{i \neq k} \mathbf{h}_k^H y_i y_i^* \mathbf{h}_k \right) \mathbf{w}_k \\ &\quad + \mathbf{n}^H (\mathbf{P}^\perp)^H \mathbf{h}_k^H y_k y_k^* \mathbf{h}_k \mathbf{P}^\perp \mathbf{n} + \sigma_k^2 y_k^* y_k. \end{aligned} \quad (32)$$

To address the optimization efficiently, we adopt the non-homogeneous quadratic transform, a recent advancement in FP that outperforms the classical QT in convergence and efficiency [30]. Inspired by the non-homogeneous bounding approach from majorization-minimization theory [69], this method eliminates costly matrix inverse operations, making it particularly suitable for large-scale wireless systems with massive antenna arrays. Therefore, to derive an upper bound

for this expression, we apply the upper-bounding identity as follows

$$\begin{aligned} &\mathbf{w}_k^H \left(\mathbf{h}_k^H y_k y_k^* \mathbf{h}_k + \sum_{i \neq k} \mathbf{h}_k^H y_i y_i^* \mathbf{h}_k \right) \mathbf{w}_k \\ &\leq \kappa_k \mathbf{w}_k^H \mathbf{w}_k + 2\text{Re} \left\{ \mathbf{w}_k^H \left(\left(\mathbf{h}_k^H y_k y_k^* \mathbf{h}_k + \sum_{i \neq k} \mathbf{h}_k^H y_i y_i^* \mathbf{h}_k \right) - \kappa_k \mathbf{I} \right) \mathbf{z}_k \right\} + \mathbf{z}_k^H \left(\kappa_k \mathbf{I} - \left(\mathbf{h}_k^H y_k y_k^* \mathbf{h}_k + \sum_{i \neq k} \mathbf{h}_k^H y_i y_i^* \mathbf{h}_k \right) \right) \mathbf{z}_k, \end{aligned} \quad (33)$$

with $\mathbf{z}_k \in \mathbb{C}^{N_t \times 1}$ being an auxiliary variable and κ_k is a tunable hyperparameter that can be chosen such that

$$\kappa_k \geq \kappa_{\max}(\mathbf{D}_k),$$

in which $\kappa_{\max}(\mathbf{D}_k)$ denotes the maximum eigenvalue of the matrix $\mathbf{D}_k \in \mathbb{C}^{N_t \times N_t}$ defined as

$$\mathbf{D}_k = \mu_k (1 + \zeta_k) \mathbf{h}_k^H y_k y_k^* \mathbf{h}_k + \sum_{i \neq k} \mu_i (1 + \zeta_i) \mathbf{h}_k^H y_i y_i^* \mathbf{h}_k. \quad (34)$$

It should be noted that equality holds if

$$\mathbf{w}_k = \mathbf{z}_k. \quad (35)$$

This leads us to the equivalent quadratic dual for the optimization problem in equation (30), given by

$$\begin{aligned} f_k(\mathbf{w}_k, y_k, \mathbf{z}_k, \zeta_k) &= \sum_{k=1}^K \mu_k (1 + \zeta_k) \left(2\text{Re}\{y_k^* \mathbf{h}_k \mathbf{w}_k\} - \left(\kappa_k \mathbf{w}_k^H \mathbf{w}_k + 2\text{Re} \left\{ \mathbf{w}_k^H \left(\left(\mathbf{h}_k^H y_k y_k^* \mathbf{h}_k + \sum_{i \neq k} \mathbf{h}_k^H y_i y_i^* \mathbf{h}_k \right) - \kappa_k \mathbf{I}_{N_t} \right) \mathbf{z}_k \right\} \right. \right. \\ &\quad \left. \left. + \mathbf{z}_k^H \left(\kappa_k \mathbf{I}_{N_t} - \left(\mathbf{h}_k^H y_k y_k^* \mathbf{h}_k + \sum_{i \neq k} \mathbf{h}_k^H y_i y_i^* \mathbf{h}_k \right) \right) \mathbf{z}_k + \mathbf{n}^H (\mathbf{P}^\perp)^H \mathbf{h}_k^H y_k y_k^* \mathbf{h}_k \mathbf{P}^\perp \mathbf{n} \right. \right. \\ &\quad \left. \left. + \sigma_k^2 y_k^* y_k \right) \right) + \sum_{k=1}^K \mu_k [\log_2(1 + \zeta_k) - \zeta_k]. \end{aligned} \quad (36)$$

Simplifying equation (36) using equation (34) results in

$$\begin{aligned} f_k(\mathbf{w}_k, y_k, \mathbf{z}_k, \zeta_k) &= \sum_{k=1}^K \left(2\text{Re}\{ \mu_k (1 + \zeta_k) y_k^* \mathbf{h}_k \mathbf{w}_k + \mathbf{w}_k^H (\kappa_k \mathbf{I}_{N_t} - \mathbf{D}_k) \mathbf{z}_k \} \right. \\ &\quad \left. + \mathbf{z}_k^H (\mathbf{D}_k - \kappa_k \mathbf{I}_{N_t}) \mathbf{z}_k - \kappa_k \mathbf{w}_k^H \mathbf{w}_k - \mu_k (1 + \zeta_k) \mathbf{n}^H (\mathbf{P}^\perp)^H \mathbf{h}_k^H y_k y_k^* \mathbf{h}_k \mathbf{P}^\perp \mathbf{n} \right. \\ &\quad \left. - \mu_k (1 + \zeta_k) \sigma_k^2 y_k^* y_k \right) + \sum_{k=1}^K \mu_k [\log_2(1 + \zeta_k) - \zeta_k]. \end{aligned} \quad (37)$$

To solve this optimization problem, we initialize by setting

$$\mathbf{z}_k^* = \mathbf{w}_k. \quad (38)$$

Next, we derive the closed-form optimum of y_k , for all k . For this process, we treat \mathbf{w}_k and ζ as constants while

optimizing with respect to y_k . This allows us to focus on the terms in $f_k(\mathbf{w}_k, y_k, \mathbf{z}_k, \zeta_k)$ that involve \mathbf{y} , given by

$$f_k(\mathbf{y}) = \sum_{k=1}^K \mu_k (1 + \zeta_k) \times \left(2 \operatorname{Re} \{ y_k^* e_k(\mathbf{w}_k) \} - y_k^* \hat{B}_k(\mathbf{w}_k) y_k \right) + c_k, \quad (39)$$

where c_k is a constant independent of \mathbf{y} . Leveraging the latter, the optimal auxiliary variable y_k^* is given by

$$y_k^* = \hat{B}_k^{-1}(\mathbf{w}_k) e_k(\mathbf{w}_k). \quad (40)$$

After substituting \mathbf{z}_k^* and y_k^* into $f_k(\mathbf{w}_k, y_k, \mathbf{z}_k, \zeta_k)$, we can solve for the optimal ζ_k by setting

$$\frac{\partial f_k(\mathbf{w}_k, y_k, \mathbf{z}_k, \zeta_k)}{\partial \zeta_k} = 0.$$

This, in turn, yields

$$\zeta_k^* = \frac{1}{\ln(2) (1 + \tilde{n}_k + \sigma_k^2 y_k y_k^* - \operatorname{Re}(y_k e_k(\mathbf{w}_k)))} - 1. \quad (41)$$

where $\tilde{n}_k \triangleq \mathbf{n}^H (\mathbf{P}^\perp)^H \mathbf{h}_k^H y_k^* y_k \mathbf{h}_k \mathbf{P}^\perp \mathbf{n}$.

Finally, we can express the updated weight \mathbf{w}_k^* as

$$\mathbf{w}_k^* = \mathbf{z}_k^* + \frac{1}{\kappa_k} (\mu_k (1 + \zeta_k^*) \mathbf{h}_k^H y_k^* - \mathbf{D}_k \mathbf{z}_k^*), \quad (42)$$

with the n -th iteration given by

$$\hat{\mathbf{w}}_k^{(n)} = \mathcal{P}_{\mathbf{w}_k \in \mathcal{W}_k} \left(\mathbf{z}_k^* + \frac{1}{\kappa_k} (\mu_k (1 + \zeta_k^*) \mathbf{h}_k^H y_k^* - \mathbf{D}_k \mathbf{z}_k^*) \right), \quad (43)$$

where $\mathcal{P}_{\mathbf{w}_k \in \mathcal{W}_k}$ denotes projection onto the feasible set \mathcal{W}_k .

B. Subproblem II: Non-homogeneous QT for AN Design

Next, let us consider the optimization over \mathbf{n} , under the assumption that \mathbf{w}_k is fixed. Then, the resulting objective function to maximize is given by

$$\max_{\mathbf{n}} \sum_{k=1}^K \mu_k \log_2 \left(1 + \frac{\mathbf{h}_k \mathbf{w}_k \mathbf{w}_k^H \mathbf{h}_k^H}{\sum_{i \neq k} \mathbf{h}_k \mathbf{w}_i \mathbf{w}_i^H \mathbf{h}_k^H + \mathbf{h}_k \mathbf{n}_{\text{eff}} \mathbf{n}_{\text{eff}}^H \mathbf{h}_k^H + \sigma_k^2} \right)$$

subject to:

$$\begin{aligned} (a) \quad & \operatorname{Tr}(\mathbf{P}^\perp \mathbf{n} \mathbf{n}^H (\mathbf{P}^\perp)^H) + \sum_{k=1}^K P_k \leq P_A, \\ (b) \quad & \mathbf{a}^H(\theta_j) \tilde{\mathbf{W}} \mathbf{a}(\theta_j) \alpha_j \geq \eta_j, \quad \forall j, \\ (c) \quad & \mathbf{a}^H(\theta_j \pm \theta_0) \tilde{\mathbf{W}} \mathbf{a}(\theta_j \pm \theta_0) \alpha_j \leq \frac{\eta_j}{2}, \quad \forall j. \end{aligned} \quad (44)$$

Leveraging a procedure similar to the previous sub-optimization, the objective function with respect to \mathbf{n} can be equivalently stated as

$$h(\mathbf{n}, \tilde{\zeta}) = \sum_{k=1}^K \tilde{\mu}_k \left[\log_2 (1 + \tilde{\zeta}_k) - \tilde{\zeta}_k + (1 + \tilde{\zeta}_k) e_k^* (e_k e_k^* + B_k(\mathbf{n}))^{-1} e_k \right], \quad (45)$$

where $\tilde{\zeta} \triangleq \{\tilde{\zeta}_1, \dots, \tilde{\zeta}_K\}$ denotes a set of auxiliary variables and we drop the inherent dependance of \mathbf{w}_k on $e_k(\mathbf{w}_k)$ and hereafter denote it as e_k . In addition, $B_k(\mathbf{n})$ is identical to $B_k(\mathbf{w}_k)$ defined in equation (26) with the implicit dependence on \mathbf{n} highlighted instead.

Next, by letting $M_k(\mathbf{n})$ to be identical to $M_k(\mathbf{w}_k)$ in equation (25) with the emphasis on \mathbf{n} , we can define $\hat{B}_k(\mathbf{n}) \triangleq e_k e_k^* + B_k(\mathbf{n})$ and $\hat{M}_k(\mathbf{n}) \triangleq e_k^* (e_k e_k^* + B_k(\mathbf{n}))^{-1} e_k$. Based on the dual complex QT, we can also rewrite $e_k^* \hat{B}_k^{-1}(\mathbf{n}) e_k$ as $2 \operatorname{Re} \{ \tilde{y}_k^* e_k \} - \tilde{y}_k^* \hat{B}_k(\mathbf{n}) \tilde{y}_k$, where $\tilde{y}_k \in \mathbb{C}$ is an auxiliary variable, which yields the optimization problem

$$\max_{\mathbf{n}, \tilde{\zeta}} h(\mathbf{n}, \tilde{\zeta}) = \sum_{k=1}^K \tilde{\mu}_k \left[\log_2 (1 + \tilde{\zeta}_k) - \tilde{\zeta}_k + (1 + \tilde{\zeta}_k) \hat{M}_k(\mathbf{n}) \right]$$

subject to:

$$\begin{aligned} (a) \quad & \operatorname{Tr}(\mathbf{P}^\perp \mathbf{n} \mathbf{n}^H (\mathbf{P}^\perp)^H) + \sum_{k=1}^K P_k \leq P_A, \\ (b) \quad & \mathbf{a}^H(\theta_j) \tilde{\mathbf{W}} \mathbf{a}(\theta_j) \alpha_j \geq \eta_j, \quad \forall j, \\ (c) \quad & \mathbf{a}^H(\theta_j \pm \theta_0) \tilde{\mathbf{W}} \mathbf{a}(\theta_j \pm \theta_0) \alpha_j \leq \frac{\eta_j}{2}, \quad \forall j, \end{aligned} \quad (46)$$

where the objective function can be rewritten as

$$f_r(\mathbf{n}, \tilde{y}_k, \tilde{\zeta}) = \sum_{k=1}^K \tilde{\mu}_k \left[(1 + \tilde{\zeta}_k) \left(2 \operatorname{Re} \{ \tilde{y}_k^* e_k \} - \tilde{y}_k^* \hat{B}_k(\mathbf{n}) \tilde{y}_k \right) + \log_2 (1 + \tilde{\zeta}_k) - \tilde{\zeta}_k \right]. \quad (47)$$

Next, following equation (32), we have

$$\begin{aligned} y_k^* \hat{B}_k(\mathbf{n}) y_k &= \mathbf{w}_k^H \left(\mathbf{h}_k^H y_k y_k^* \mathbf{h}_k + \sum_{i \neq k} \mathbf{h}_k^H y_i y_i^* \mathbf{h}_k \right) \mathbf{w}_k \\ &+ \mathbf{n}^H (\mathbf{P}^\perp)^H \mathbf{h}_k^H y_k y_k^* \mathbf{h}_k \mathbf{P}^\perp \mathbf{n} + \sigma_k^2 y_k^* y_k. \end{aligned} \quad (48)$$

In addition, inspired by the non-homogeneous bounding approach [69], the second term in equation (48) can be upper bounded as

$$\begin{aligned} & \mathbf{n}^H ((\mathbf{P}^\perp)^H \mathbf{h}_k^H \tilde{y}_k \tilde{y}_k^* \mathbf{h}_k \mathbf{P}^\perp) \mathbf{n} \\ & \leq \tilde{\kappa}_k \mathbf{n}^H \mathbf{n} + 2 \operatorname{Re} \{ \mathbf{n}^H ((\mathbf{P}^\perp)^H \mathbf{h}_k^H \tilde{y}_k \tilde{y}_k^* \mathbf{h}_k \mathbf{P}^\perp) \mathbf{z} \} \\ & + \mathbf{z}^H (\tilde{\kappa}_k \mathbf{I} - ((\mathbf{P}^\perp)^H \mathbf{h}_k^H \tilde{y}_k \tilde{y}_k^* \mathbf{h}_k \mathbf{P}^\perp)) \mathbf{z}, \end{aligned} \quad (49)$$

where $\mathbf{z} \in \mathbb{C}^{N_t \times 1}$ is an auxiliary variable, and the equality holds if $\mathbf{n} = \mathbf{z}$. $\tilde{\kappa}_k$ is a tunable hyperparameter that can be chosen such that

$$\tilde{\kappa}_k \geq \tilde{\kappa}_{\max}(\tilde{\mathbf{D}}_k),$$

in which $\tilde{\kappa}_{\max}(\tilde{\mathbf{D}}_k)$ denotes the maximum eigenvalue of the matrix $\tilde{\mathbf{D}}_k \in \mathbb{C}^{N_t \times N_t}$ defined as

$$\tilde{\mathbf{D}}_k \triangleq \tilde{\mu}_k (1 + \tilde{\zeta}_k) ((\mathbf{P}^\perp)^H \mathbf{h}_k^H \tilde{y}_k \tilde{y}_k^* \mathbf{h}_k \mathbf{P}^\perp). \quad (50)$$

Therefore, the equivalent quadratic dual for the optimization

problem defined in equation (46) becomes

$$\begin{aligned}
f_r(\mathbf{n}, \tilde{y}_k, \mathbf{z}, \tilde{\zeta}) = & \sum_{k=1}^K \tilde{\mu}_k (1 + \tilde{\zeta}_k) \left(2 \operatorname{Re} \{ \tilde{y}_k^* \mathbf{h}_k \mathbf{w}_k \} - \left(\tilde{\kappa}_k \mathbf{n}^H \mathbf{n} \right. \right. \\
& + 2 \operatorname{Re} \{ \mathbf{n}^H ((\mathbf{P}^\perp)^H \mathbf{h}_k^H \tilde{y}_k \tilde{y}_k^* \mathbf{h}_k \mathbf{P}^\perp) - \tilde{\kappa}_k \mathbf{I} \} \mathbf{z} \} \\
& + \mathbf{z}^H (\tilde{\kappa}_k \mathbf{I} - ((\mathbf{P}^\perp)^H \mathbf{h}_k^H \tilde{y}_k \tilde{y}_k^* \mathbf{h}_k \mathbf{P}^\perp)) \mathbf{z} \\
& + \mathbf{w}_k^H \left(\mathbf{h}_k^H \tilde{y}_k \tilde{y}_k^* \mathbf{h}_k + \sum_{i \neq k} \mathbf{h}_k^H \tilde{y}_i \tilde{y}_i^* \mathbf{h}_k \right) \mathbf{w}_k + \sigma_k^2 \tilde{y}_k^* \tilde{y}_k \Big) \Big) \\
& + \sum_{k=1}^K \tilde{\mu}_k \left[\log_2(1 + \tilde{\zeta}_k) - \tilde{\zeta}_k \right]. \tag{51}
\end{aligned}$$

Next, simplifying equation (51) using equation (50) yields

$$\begin{aligned}
f_r(\mathbf{n}, \tilde{y}_k, \mathbf{z}, \tilde{\zeta}) = & \sum_{k=1}^K \left(2 \operatorname{Re} \{ \tilde{\mu}_k (1 + \tilde{\zeta}_k) \tilde{y}_k^* \mathbf{h}_k \mathbf{w}_k + \mathbf{n}^H (\tilde{\kappa}_k \mathbf{I} - \tilde{\mathbf{D}}_k) \mathbf{z} \} \right. \\
& + \mathbf{z}^H (\tilde{\mathbf{D}}_k - \tilde{\kappa}_k \mathbf{I}) \mathbf{z} - \tilde{\kappa}_k \mathbf{n}^H \mathbf{n} \\
& - \tilde{\mu}_k (1 + \tilde{\zeta}_k) \mathbf{w}_k^H \left(\mathbf{h}_k^H \tilde{y}_k \tilde{y}_k^* \mathbf{h}_k + \sum_{i \neq k} \mathbf{h}_k^H \tilde{y}_i \tilde{y}_i^* \mathbf{h}_k \right) \mathbf{w}_k \\
& \left. - \tilde{\mu}_k (1 + \tilde{\zeta}_k) \sigma_k^2 \tilde{y}_k^* \tilde{y}_k \right) + \sum_{k=1}^K \tilde{\mu}_k \left[\log_2(1 + \tilde{\zeta}_k) - \tilde{\zeta}_k \right]. \tag{52}
\end{aligned}$$

To solve this optimization problem, we first set

$$\mathbf{z}^* = \mathbf{n}. \tag{53}$$

Next, to compute the closed-form optimal value of \tilde{y}_k , we fix \mathbf{n} and $\tilde{\zeta}_k$ to optimize with respect to \tilde{y}_k , treating the other variables as constants. Given this setup, we can proceed by focusing solely on the terms in $f_r(\mathbf{n}, \tilde{y}_k, \mathbf{z}, \tilde{\zeta})$ that involve \tilde{y}_k to find the closed-form expression for the optimal \tilde{y}_k^* .

The objective function with respect to \tilde{y}_k can be expressed as

$$f_r(\tilde{y}_k) = \tilde{\mu}_k (1 + \tilde{\zeta}_k) \left(2 \operatorname{Re} \{ \tilde{y}_k^* e_k \} - \tilde{y}_k^* \hat{B}_k(\mathbf{n}) \tilde{y}_k \right) + c_r, \tag{54}$$

where c_r is a constant independent of \tilde{y}_k .

Therefore, the optimal auxiliary variable \tilde{y}_k^* is given by

$$\tilde{y}_k^* = \hat{B}_k^{-1}(\mathbf{n}) e_k. \tag{55}$$

Substituting \mathbf{z}^* and \tilde{y}_k^* into $f_r(\mathbf{n}, \tilde{y}_k, \mathbf{z}, \tilde{\zeta}_k)$, we can solve for the optimal $\tilde{\zeta}_k^*$ by solving

$$\frac{\partial f_r(\mathbf{n}, \tilde{y}_k, \mathbf{z}, \tilde{\zeta}_k)}{\partial \tilde{\zeta}_k} = 0.$$

Taking the derivative with respect to $\tilde{\zeta}_k$, we obtain

$$\begin{aligned}
\frac{\partial f_r(\tilde{\zeta}_k)}{\partial \tilde{\zeta}_k} = & \tilde{\mu}_k (2 \operatorname{Re} \{ \tilde{y}_k^* \mathbf{h}_k \mathbf{w}_k \}) \\
& - \tilde{\mu}_k \mathbf{w}_k^H \left(\mathbf{h}_k^H \tilde{y}_k \tilde{y}_k^* \mathbf{h}_k + \sum_{i \neq k} \mathbf{h}_k^H \tilde{y}_i \tilde{y}_i^* \mathbf{h}_k \right) \mathbf{w}_k \\
& - \tilde{\mu}_k \sigma_k^2 \tilde{y}_k^* \tilde{y}_k + \frac{\tilde{\mu}_k}{\ln(2)} \cdot \frac{1}{1 + \tilde{\zeta}_k} - \tilde{\mu}_k = 0. \tag{56}
\end{aligned}$$

Solving for $\tilde{\zeta}_k$ yields

$$\begin{aligned}
\tilde{\zeta}_k^* = & \frac{1}{\ln(2)} \left[\mathbf{w}_k^H \left(\mathbf{h}_k^H \tilde{y}_k \tilde{y}_k^* \mathbf{h}_k + \sum_{i \neq k} \mathbf{h}_k^H \tilde{y}_i \tilde{y}_i^* \mathbf{h}_k \right) \mathbf{w}_k \right. \\
& \left. + \sigma_k^2 \tilde{y}_k^* \tilde{y}_k - 2 \operatorname{Re} \{ \tilde{y}_k^* \mathbf{h}_k \mathbf{w}_k \} \right]^{-1} - 1. \tag{57}
\end{aligned}$$

Finally, aggregating the terms involving \mathbf{n} yields

$$f_r(\mathbf{n}) = \sum_{k=1}^K (2 \operatorname{Re} \{ \mathbf{n}^H (\tilde{\kappa}_k \mathbf{I} - \mathbf{D}_k) \mathbf{z} \} - \tilde{\kappa}_k \mathbf{n}^H \mathbf{n}).$$

Let

$$\mathbf{M} = \sum_{k=1}^K \tilde{\kappa}_k \mathbf{I}, \quad \mathbf{B} = \sum_{k=1}^K (\tilde{\kappa}_k \mathbf{I} - \mathbf{D}_k) \mathbf{z}.$$

Then, the simplified objective for \mathbf{n} becomes

$$f_r(\mathbf{n}) = 2 \operatorname{Re} \{ \mathbf{n}^H \mathbf{B} \} - \mathbf{n}^H \mathbf{M} \mathbf{n}.$$

The derivative with respect to \mathbf{n}^H can be calculated as

$$\frac{\partial f_r(\mathbf{n})}{\partial \mathbf{n}^H} = 2 \mathbf{B} - 2 \mathbf{M} \mathbf{n}.$$

Setting the derivative to zero yields

$$\mathbf{M} \mathbf{n} = \mathbf{B}.$$

This trivially leads to

$$\mathbf{n}^* = \mathbf{M}^{-1} \mathbf{B} = \left(\sum_{k=1}^K \tilde{\kappa}_k \mathbf{I} \right)^{-1} \sum_{k=1}^K (\tilde{\kappa}_k \mathbf{I} - \mathbf{D}_k) \mathbf{z}. \tag{58}$$

This solution now ensures consistency across all K terms, yielding a unified \mathbf{n}^* , for which the t -th iteration is given by

$$\hat{\mathbf{n}}^{(t)} = \mathcal{P}_{\mathbf{n} \in \mathcal{N}} \left(\left(\sum_{k=1}^K \tilde{\kappa}_k \mathbf{I} \right)^{-1} \sum_{k=1}^K (\tilde{\kappa}_k \mathbf{I} - \mathbf{D}_k) \mathbf{n}^{t-1} \right), \tag{59}$$

where $\mathcal{P}_{\mathbf{n} \in \mathcal{N}}$ denotes the projection onto the feasible set \mathcal{N} .

The complete executable steps for the proposed approach are summarized in Algorithm 2.

Algorithm 2 Proposed Secure ISAC Algorithm

- 1: **Input:** Vector $\boldsymbol{\mu}$
 - 2: Initialize \mathbf{w} and \mathbf{n} to a feasible value based on the related constraints
 - 3: **repeat**
 - 4: **Optimization Problem 1** (\mathbf{n} is held fixed)
 - 5: **for** each k **do**
 - 6: Update auxiliary variable \mathbf{z}_k according to eq. (38).
 - 7: Update auxiliary variable \mathbf{y}_k according to eq. (40).
 - 8: Update auxiliary variable $\tilde{\zeta}_k$ according to eq. (41).
 - 9: Update decision variable \mathbf{w}_k according to eq. (42).
 - 10: Update gradient projection \mathbf{w}_k from eq. (43).
 - 11: **end for**
 - 12: **Optimization Problem 2** (\mathbf{w}_k is held fixed)
 - 13: Update auxiliary variable \mathbf{z}_k according to eq. (53).
 - 14: Update auxiliary variable \tilde{y}_k according to eq. (54).
 - 15: Update auxiliary variable $\tilde{\zeta}_k$ according to eq. (57).
 - 16: Update decision variable \mathbf{n} according to eq. (58).
 - 17: **until** the objective function in (16) converges
-

V. PERFORMANCE ANALYSIS

To assess the performance of the proposed approaches, this section presents numerical results obtained via Monte Carlo simulations. These results are used to demonstrate the effectiveness of the developed beamforming and artificial noise design. Without loss of generality, the entries of the channel matrix \mathbf{h}_k are modeled as independent and identically distributed (i.i.d.) complex Gaussian random variables following $\mathbf{h}_k \sim \mathcal{CN}(0, 1)$. The ISAC base station is assumed to employ a uniform linear array (ULA) with half-wavelength spacing between antenna elements. For simplicity, the noise variance at the targets is assumed to match that of the intended CUs. The parameters used for the analysis are summarized below in Table I.

First, Fig. 2 presents results for the average secrecy rate for a varying number user equipments (UEs), eavesdroppers, and transmit antennas. As highlighted in the aforementioned figure, the average secrecy rate increases when the number of transmit antennas increases due to the larger number of degrees-of-freedom (DoF) available in the system, while having more eavesdroppers and more users decreases the secrecy rate as a whole. In addition, the proposed method outperforms the SotA work done in [1] across all SNRs with a large gain of more than 10 dB, due to the flooring of the SotA technique, an average secrecy rate of around 4 bit/s/Hz.

Next, Fig. 3 presents the performance of the proposed Algorithm 2 in terms of the average data rate as a metric for evaluating the communications performance of the system.

A similar trend to the average secrecy rate in Fig. 2 is seen here as the average data rate increases when the number of transmit antennas increase due to the larger number of DoF available in the system, while having more eavesdroppers and more users decreases the secrecy rate as a whole. In addition, the average data rate is almost identical to the average secrecy rate, which means that very little data is leaked to eavesdroppers according to equation (4), with the users achieving almost a full rate within the system.

Figure 4 illustrates the sensing performance by showing the beam gain across various eavesdropper directions of interest. The SINR threshold for each legitimate user is fixed at 20 dB. For reference, a narrow beam pattern, assuming perfect knowledge of the target direction at the base station, is used as a benchmark.

TABLE I
SIMULATION PARAMETERS FOR JOINT OPTIMIZATION

Parameter	Symbol	Value
Number of users	K	2, 4, 8
Number of eavesdroppers	J	1, 2
Transmit antennas	N_T	8, 16, 18
Total available power	P_A	20 dBm
Direction of eavesdroppers	θ_j	$[-90^\circ, +90^\circ]$
Mainlobe leakage range	θ_0	$[0^\circ, 20^\circ]$
Secrecy SINR threshold	β_j	0.1
Minimum sensing gain	η_j	2
Path loss (eavesdropper)	α_j	1
Fairness constraint threshold	ξ_F	0.5
Entropy regularization weight	ν	0.01

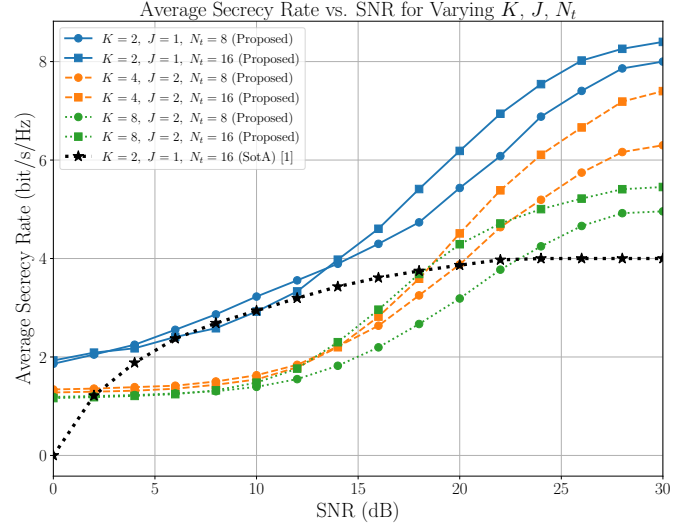


Fig. 2. Average Secrecy Rate performance of the proposed Algorithm 2 under varying numbers of users K , targets J , and transmit antennas N_t , compared with a representative SotA method.

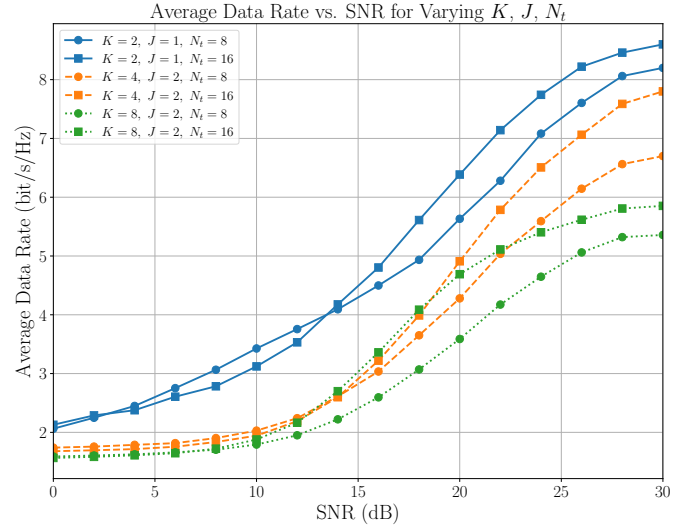


Fig. 3. Average Data Rate performance of the proposed Algorithm 2 under varying numbers of users K , targets J , and transmit antennas N_t .

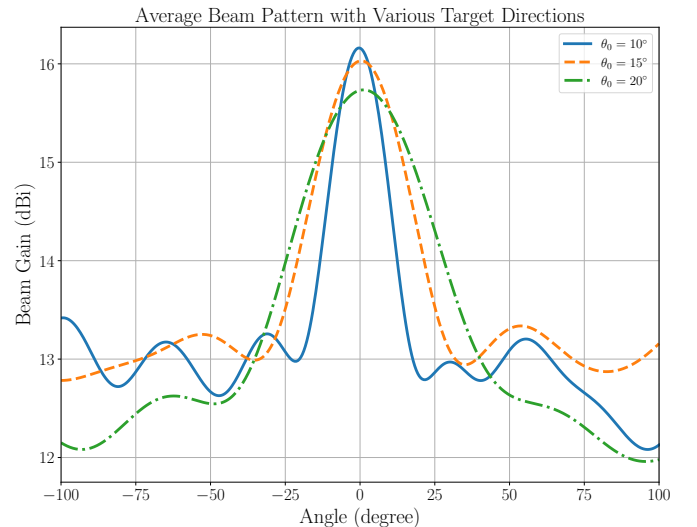


Fig. 4. Beam Gain of the proposed Algorithm 2 for various target directions with $N_t = 16$, $K = 4$ and $J = 1$.

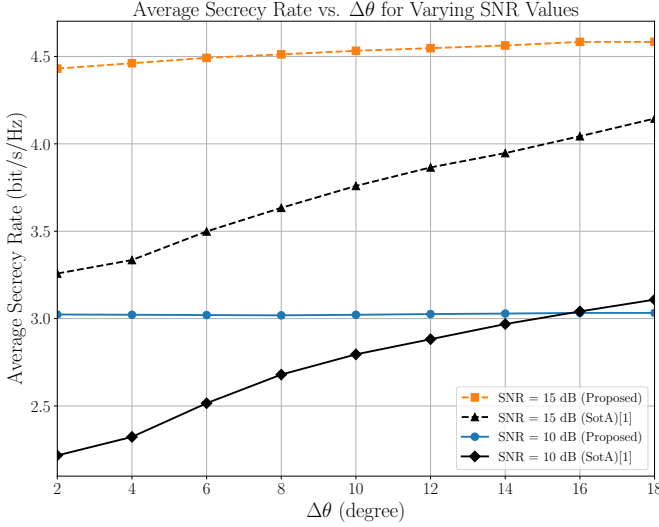


Fig. 5. Average Secrecy Rate performance vs. varying angles of the proposed Algorithm 2 with $N_t = 18$, $K = 4$ and $J = 1$.

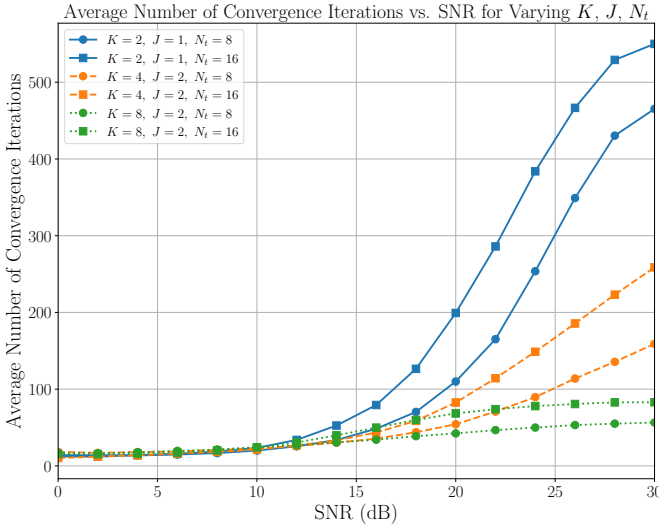


Fig. 6. Convergence behavior of the proposed Algorithm 2 under a varying K , J and N_t .

In contrast, the proposed algorithms produce wide main-lobe beam patterns that deliver consistent power levels across the entire angular range from -90° to $+90^\circ$, enabling robust sensing. While some reduction in beam gain is observed as the region of interest widens, the results confirm that high gains are preserved even for $\theta_0 = 20^\circ$, indicating reliable detection performance over a broad angular span.

Additionally, Fig. 5 illustrates how the average secrecy rate varies with respect to changes in $\Delta\theta$. As evident from the figure, the proposed algorithm consistently outperforms the SotA across all values of $\Delta\theta$, achieving a higher average secrecy rate throughout. Notably, thanks to the integration of artificial noise, the proposed method exhibits a more stable performance as $\Delta\theta$ increases, in contrast to the significant fluctuations observed in the SotA.

Finally, Fig. 6 presents the convergence behavior of the proposed algorithm. Due to the alternating nature of the proposed algorithm, the algorithm converges much faster for larger systems due to the larger number of DoFs in the solution space, while smaller systems require a much larger number of iterations to converge.

VI. CONCLUSION

This work presented a novel secure MU-ISAC framework that jointly maximizes secrecy rate under communication and sensing constraints while promoting user fairness via an entropy-regularized Jain's index. To solve the resulting non-convex problem, we proposed an efficient dual fractional programming method based on a non-homogeneous quadratic transform, enabling closed-form, scalable optimization of secure beamforming and artificial noise. We further introduced an iterative fairness-throughput tradeoff scheme to analyze system behavior across operating regimes. Simulation results corroborate the effectiveness of the proposed approach, demonstrating substantial performance gains in terms of average secrecy rate, data throughput, and beamforming accuracy, thus highlighting its suitability for secure and fair ISAC system design.

ACKNOWLEDGMENT

This work was funded by the German Federal Ministry of Education and Research (grant 16KISK231), the German Research Foundation (Germany's Excellence Strategy-EXC2050/1-ProjectID 390696704-Cluster of Excellence CeTI of Dresden, University of Technology), and based on the budget passed by the Saxon State Parliament.

REFERENCES

- [1] N. Su, F. Liu, and C. Masouros, "Secure radar-communication systems with malicious targets: Integrating radar, communications and jamming functionalities," *IEEE Transactions on Wireless Communications*, vol. 20, no. 1, pp. 83–95, 2021.
- [2] F. Dong, W. Wang, X. Li, F. Liu, S. Chen, and L. Hanzo, "Joint beamforming design for dual-functional MIMO radar and communication systems guaranteeing physical layer security," *IEEE Transactions on Green Communications and Networking*, vol. 7, no. 1, pp. 537–549, 2023.
- [3] J. Zhang, S. Wang, Z. Zheng, Z. Fei, H. Yu, Q. Zhang, and Z. Han, "Enhancing performance of integrated sensing and communication via joint optimization of hybrid and passive reconfigurable intelligent surfaces," *IEEE Internet of Things Journal*, vol. 11, no. 19, pp. 32 041–32 054, 2024.
- [4] Z. Wei, F. Liu, C. Masouros, N. Su, and A. P. Petropulu, "Toward multifunctional 6G wireless networks: Integrating sensing, communication, and security," *IEEE Communications Magazine*, vol. 60, no. 4, pp. 65–71, 2022.
- [5] Z. Ren, L. Qiu, J. Xu, and D. W. K. Ng, "Robust transmit beamforming for secure integrated sensing and communication," *IEEE Transactions on Communications*, vol. 71, no. 9, pp. 5549–5564, 2023.
- [6] H. Peng, C. He, Z. Zhang, C. Han, and L. Wang, "Robust secure beamforming for integrated sensing and communication systems with the active RIS," *IEEE Transactions on Vehicular Technology*, vol. 74, no. 3, pp. 5158–5163, 2025.
- [7] Z. Wei, H. Qu, Y. Wang, X. Yuan, H. Wu, Y. Du, K. Han, N. Zhang, and Z. Feng, "Integrated sensing and communication signals toward 5G-A and 6G: A survey," *IEEE Internet of Things Journal*, vol. 10, no. 13, pp. 11 068–11 092, 2023.
- [8] Y. Li, F. Khan, M. Ahmed, A. A. Soofi, W. U. Khan, C. K. Sheemar, M. Asif, and Z. Han, "RIS-based physical layer security for integrated sensing and communication: A comprehensive survey," *IEEE Internet of Things Journal*, pp. 1–1, 2025.
- [9] W. Zhu, H. D. Tuan, E. Dutkiewicz, Y. Fang, H. V. Poor, and L. Hanzo, "Long-term rate-fairness-aware beamforming based massive MIMO systems," *IEEE Transactions on Communications*, vol. 72, no. 4, pp. 2386–2398, 2024.
- [10] I. A. M. Sandoval, K. Ando, O. Taghizadeh, and G. T. F. De Abreu, "Sum-rate maximization and leakage minimization for multi-user cell-free massive MIMO systems," *IEEE Access*, vol. 11, pp. 127 509–127 525, 2023.

- [11] Y. Zhuo, T. Mao, H. Li, C. Sun, Z. Wang, Z. Han, and S. Chen, "Multi-beam integrated sensing and communication: State-of-the-art, challenges and opportunities," *IEEE Communications Magazine*, vol. 62, no. 9, pp. 90–96, 2024.
- [12] A. Deligiannis, A. Daniyan, S. Lambbotharan, and J. A. Chambers, "Secrecy rate optimizations for MIMO communication radar," *IEEE Transactions on Aerospace and Electronic Systems*, vol. 54, no. 5, pp. 2481–2492, 2018.
- [13] J. Chu, R. Liu, M. Li, Y. Liu, and Q. Liu, "Joint secure transmit beamforming designs for integrated sensing and communication systems," *IEEE Transactions on Vehicular Technology*, vol. 72, no. 4, pp. 4778–4791, 2023.
- [14] M. Mitev, A. Mayya, and A. Chorti, *Joint Secure Communication and Sensing in 6G Networks*, 2024, pp. 203–220.
- [15] B. Zhao, T. Qiu, G. Ren, Z. Jin, and Z. Liu, "RSMA-enhanced physical layer security for ISAC systems," *IEEE Wireless Communications Letters*, vol. 14, no. 4, pp. 1064–1068, 2025.
- [16] T. Xu, Y. Ye, and C. Masouros, "Signal waveform design for resilient integrated sensing and communications," in *2024 14th International Symposium on Communication Systems, Networks and Digital Signal Processing (CSNDSP)*, 2024, pp. 109–114.
- [17] A. K. Boroujeni, G. T. F. de Abreu, S. Köpsell, G. Bagheri, K. R. R. Ranasinghe, and R. F. Schaefer, "Frequency hopping waveform design for secure integrated sensing and communications," 2025. [Online]. Available: <https://arxiv.org/abs/2504.10052>
- [18] O. Günlü, M. R. Bloch, R. F. Schaefer, and A. Yener, "Secure integrated sensing and communication," *IEEE Journal on Selected Areas in Information Theory*, vol. 4, pp. 40–53, 2023.
- [19] A. Agarwal and K. Singh, "Fairness driven joint phase and pac optimization for NOMA transmission with D/ND-IRS," *IEEE Transactions on Vehicular Technology*, pp. 1–12, 2025.
- [20] H.-J. Chou, C.-J. Tsao, J.-M. Wu, J.-Y. Hsu, and P.-A. Ting, "Fair resource allocation for multiuser MIMO communications network," in *2014 IEEE Global Communications Conference*, 2014, pp. 3910–3915.
- [21] E. Shtaiwi, H. Zhang, A. Abdelhadi, A. L. Swindlehurst, Z. Han, and H. V. Poor, "Sum-rate maximization for RIS-assisted integrated sensing and communication systems with manifold optimization," *IEEE Transactions on Communications*, vol. 71, no. 8, pp. 4909–4923, 2023.
- [22] J. Singh, A. K. Jagannatham, and L. Hanzo, "Geometric mean rate maximization in RIS-aided mmWave ISAC systems relying on a non-diagonal phase shift matrix," *IEEE Open Journal of the Communications Society*, vol. 6, pp. 4756–4771, 2025.
- [23] R. Jain, D. M. Chiu, and H. W. R., "A quantitative measure of fairness and discrimination for resource allocation in shared computer systems," *CoRR*, vol. cs.NI/9809099, 01 1998.
- [24] C. Dou, N. Huang, Y. Wu, L. Qian, Z. Shi, and T. Q. S. Quek, "Integrated sensing and communication enabled multidevice multitarget cooperative sensing: A fairness-aware design," *IEEE Internet of Things Journal*, vol. 11, no. 17, pp. 29 190–29 201, 2024.
- [25] Y. Xiong, F. Liu, Y. Cui, W. Yuan, T. X. Han, and G. Caire, "On the fundamental tradeoff of integrated sensing and communications under gaussian channels," *IEEE Transactions on Information Theory*, vol. 69, no. 9, pp. 5723–5751, 2023.
- [26] W. Lyu, S. Yang, Y. Xiu, X. Chen, Z. Zhang, C. Assi, and C. Yuen, "Dual-robust integrated sensing and communication: Beamforming under CSI imperfection and location uncertainty," *IEEE Wireless Communications Letters*, vol. 13, no. 11, pp. 3124–3128, 2024.
- [27] X. Li, R. Yao, A.-A. A. Boulogeorgos, and T. A. Tsiftsis, "Fairness vs. equality: RSMA-based multi-target and multi-user integrated sensing and communications," 2025. [Online]. Available: <https://arxiv.org/abs/2504.03361>
- [28] T. T. Nguyen, K. Elbassioni, N. C. Luong, D. Niyato, and D. I. Kim, "Access management in joint sensing and communication systems: Efficiency versus fairness," *IEEE Transactions on Vehicular Technology*, vol. 71, no. 5, pp. 5128–5142, 2022.
- [29] K. Shen and W. Yu, "Fractional Programming for communication systems—part II: Uplink scheduling via matching," *IEEE Transactions on Signal Processing*, vol. 66, no. 10, pp. 2631–2644, 2018.
- [30] K. Shen, Z. Zhao, Y. Chen, Z. Zhang, and H. Victor Cheng, "Accelerating quadratic transform and WMMSE," *IEEE Journal on Selected Areas in Communications*, vol. 42, no. 11, pp. 3110–3124, 2024.
- [31] Q. Shi, M. Razaviyayn, Z.-Q. Luo, and C. He, "An iteratively weighted MMSE approach to distributed sum-utility maximization for a MIMO interfering broadcast channel," *IEEE Transactions on Signal Processing*, vol. 59, no. 9, pp. 4331–4340, 2011.
- [32] A. A. Khan, R. S. Adve, and W. Yu, "Optimizing downlink resource allocation in multiuser MIMO networks via fractional programming and the hungarian algorithm," *IEEE Transactions on Wireless Communications*, vol. 19, no. 8, pp. 5162–5175, 2020.
- [33] K. Shen and W. Yu, "Fractional programming for communication systems—part I: Power control and beamforming," *IEEE Transactions on Signal Processing*, vol. 66, no. 10, pp. 2616–2630, 2018.
- [34] Y. Chen, Y. Feng, X. Li, L. Zhao, and K. Shen, "Fast fractional programming for multi-cell integrated sensing and communications," in *2024 16th International Conference on Wireless Communications and Signal Processing (WCSP)*, 2024, pp. 894–899.
- [35] S. Uchimura, K. Ando, G. T. F. de Abreu, and K. Ishibashi, "Joint design of equalization and beamforming for single-carrier MIMO transmission over millimeter-wave and sub-terahertz channels," *IEEE Transactions on Wireless Communications*, vol. 24, no. 3, pp. 1978–1991, 2025.
- [36] D. Fuhrmann and G. San Antonio, "Transmit beamforming for MIMO radar systems using partial signal correlation," in *Conference Record of the Thirty-Eighth Asilomar Conference on Signals, Systems and Computers, 2004.*, vol. 1, 2004, pp. 295–299 Vol.1.
- [37] D. R. Fuhrmann and G. San Antonio, "Transmit beamforming for MIMO radar systems using signal cross-correlation," *IEEE Transactions on Aerospace and Electronic Systems*, vol. 44, no. 1, pp. 171–186, 2008.
- [38] X. Liu, T. Huang, N. Shlezinger, Y. Liu, J. Zhou, and Y. C. Eldar, "Joint transmit beamforming for multiuser MIMO communications and MIMO radar," *IEEE Transactions on Signal Processing*, vol. 68, pp. 3929–3944, 2020.
- [39] C. Qi, W. Ci, J. Zhang, and X. You, "Hybrid beamforming for millimeter wave MIMO integrated sensing and communications," *IEEE Communications Letters*, vol. 26, no. 5, pp. 1136–1140, 2022.
- [40] S. Boyd, N. Parikh, E. Chu, B. Peleato, and J. Eckstein, 2011.
- [41] M. Razaviyayn, M. Hong, and Z.-Q. Luo, "A unified convergence analysis of block successive minimization methods for nonsmooth optimization," *SIAM Journal on Optimization*, vol. 23, no. 2, pp. 1126–1153, 2013. [Online]. Available: <https://doi.org/10.1137/120891009>
- [42] S. Lu, F. Liu, Y. Li, K. Zhang, H. Huang, J. Zou, X. Li, Y. Dong, F. Dong, J. Zhu, Y. Xiong, W. Yuan, Y. Cui, and L. Hanzo, "Integrated sensing and communications: Recent advances and ten open challenges," *IEEE Internet of Things Journal*, vol. 11, no. 11, pp. 19 094–19 120, 2024.
- [43] B. Liu, S. Gao, Z. Yang, X. Cheng, and L. Yang, "Beam pattern modulation embedded hybrid transceiver optimization for integrated sensing and communication," *IEEE Transactions on Wireless Communications*, vol. 24, no. 6, pp. 4966–4980, 2025.
- [44] H. Hua, T. X. Han, and J. Xu, "MIMO integrated sensing and communication: CRB-rate tradeoff," *IEEE Transactions on Wireless Communications*, vol. 23, no. 4, pp. 2839–2854, 2024.
- [45] P. Wang, D. Han, Y. Cao, W. Ni, and D. Niyato, "Multi-objective optimization-based waveform design for multi-user and multi-target MIMO-ISAC systems," *IEEE Transactions on Wireless Communications*, vol. 23, no. 10, pp. 15 339–15 352, 2024.
- [46] S. Wang, W. Dai, H. Wang, and G. Y. Li, "Robust waveform design for integrated sensing and communication," *IEEE Transactions on Signal Processing*, vol. 72, pp. 3122–3138, 2024.
- [47] C. Meng, Z. Wei, and Z. Feng, "Adaptive waveform optimization for MIMO integrated sensing and communication systems based on mutual information," in *2022 14th International Conference on Wireless Communications and Signal Processing (WCSP)*, 2022, pp. 472–477.
- [48] X. Long, Y. Zhao, H. Wu, and C.-Z. Xu, "Deep reinforcement learning for integrated sensing and communication in RIS-assisted 6G V2X system," *IEEE Internet of Things Journal*, vol. 11, no. 24, pp. 39 834–39 849, 2024.
- [49] C. Liu, W. Yuan, S. Li, X. Liu, H. Li, D. W. K. Ng, and Y. Li, "Learning-based predictive beamforming for integrated sensing and communication in vehicular networks," *IEEE Journal on Selected Areas in Communications*, vol. 40, no. 8, pp. 2317–2334, 2022.
- [50] H. Zhang, R. Liu, M. Li, W. Wang, and Q. Liu, "Joint sensing and communication optimization in target-mounted STARS-assisted vehicular networks: A MADRL approach," *IEEE Transactions on Vehicular Technology*, vol. 73, no. 7, pp. 10 011–10 025, 2024.
- [51] N. Huang, C. Dou, Y. Wu, L. Qian, and R. Lu, "Energy-efficient integrated sensing and communication: A multi-access edge computing design," *IEEE Wireless Communications Letters*, vol. 12, no. 12, pp. 2053–2057, 2023.
- [52] Z. Liu, J. Zhang, H. Liu, and S. Yan, "Energy-efficient resource allocation scheme for integrated sensing and communications-aided vehicular networks," in *2023 IEEE 23rd International Conference on Communication Technology (ICCT)*, 2023, pp. 1503–1508.

- [53] W. Xu, Y. Xiao, A. Liu, and M. Zhao, "Joint scattering environment sensing and channel estimation for integrated sensing and communication," in *ICC 2023 - IEEE International Conference on Communications*, 2023, pp. 541–546.
- [54] Y. Xu, N. Cao, Y. Jin, H. Zhang, C. Huang, Q. Chen, and C. Yuen, "Robust beamforming design for integrated sensing and communication systems," *IEEE Journal of Selected Areas in Sensors*, vol. 1, pp. 114–123, 2024.
- [55] Z. Xiao, Y. Zeng, F. Wen, Z. Zhang, and D. W. K. Ng, "Integrated sensing and channel estimation by exploiting dual timescales for delay-doppler alignment modulation," *IEEE Transactions on Wireless Communications*, vol. 24, no. 1, pp. 415–429, 2025.
- [56] Y. Zhang, W. Ni, W. Tang, Y. C. Eldar, and D. Niyato, "Robust transceiver design for ISAC with imperfect CSI," in *GLOBECOM 2023 - 2023 IEEE Global Communications Conference*, 2023, pp. 1320–1325.
- [57] B. Liao, H. Q. Ngo, M. Matthaiou, and P. J. Smith, "Low-complexity transmit beamforming design for massive MIMO-ISAC systems," in *GLOBECOM 2023 - 2023 IEEE Global Communications Conference*, 2023, pp. 540–545.
- [58] M. Temiz and C. Masouros, "Unsupervised learning-based low-complexity integrated sensing and communication precoder design," *IEEE Open Journal of the Communications Society*, vol. 6, pp. 3543–3554, 2025.
- [59] S. Zargari, D. Galappaththige, and C. Tellambura, "Low-complexity CRB minimization for ISAC with a generalized target response matrix," *IEEE Wireless Communications Letters*, pp. 1–1, 2025.
- [60] S. P. Chepuri, N. Shlezinger, F. Liu, G. C. Alexandropoulos, S. Buzzi, and Y. C. Eldar, "Integrated sensing and communications with reconfigurable intelligent surfaces: From signal modeling to processing," *IEEE Signal Processing Magazine*, vol. 40, no. 6, pp. 41–62, 2023.
- [61] M. I. Ismail, A. M. Shaheen, M. M. Fouda, and A. S. Alwakeel, "RIS-assisted integrated sensing and communication systems: Joint reflection and beamforming design," *IEEE Open Journal of the Communications Society*, vol. 5, pp. 908–927, 2024.
- [62] P. Saikia, A. Jee, K. Singh, C. Pan, T. A. Tsiftsis, and W.-J. Huang, "RIS-aided integrated sensing and communications," in *GLOBECOM 2023 - 2023 IEEE Global Communications Conference*, 2023, pp. 5080–5085.
- [63] A. M. Elbir, K. V. Mishra, S. Chatzinotas, and M. Bennis, "Terahertz-band integrated sensing and communications: Challenges and opportunities," *IEEE Aerospace and Electronic Systems Magazine*, vol. 39, no. 12, pp. 38–49, 2024.
- [64] Y. Wu, C. Han, and Z. Chen, "THz ISCI: Terahertz integrated sensing, communication and intelligence," in *2021 46th International Conference on Infrared, Millimeter and Terahertz Waves (IRMMW-THz)*, 2021, pp. 1–2.
- [65] K. F. Haque, F. Meneghello, and F. Restuccia, "Integrated sensing and communication for efficient edge computing," in *2024 20th International Conference on Wireless and Mobile Computing, Networking and Communications (WiMob)*, 2024, pp. 611–614.
- [66] X. Zhang and Q. Zhu, "Federated learning based integrated sensing, communications, and powering over 6G massive-MIMO mobile networks," in *IEEE INFOCOM 2024 - IEEE Conference on Computer Communications Workshops (INFOCOM WKSHPS)*, 2024, pp. 1–6.
- [67] S. Tariq, B. E. Arfeto, U. Khalid, S. Kim, T. Q. Duong, and H. Shin, "Deep quantum-transformer networks for multimodal beam prediction in ISAC systems," *IEEE Internet of Things Journal*, vol. 11, no. 18, pp. 29 387–29 401, 2024.
- [68] J. Li and P. Stoica, "MIMO radar with colocated antennas," *IEEE Signal Processing Magazine*, vol. 24, no. 5, pp. 106–114, 2007.
- [69] Y. Sun, P. Babu, and D. P. Palomar, "Majorization-minimization algorithms in signal processing, communications, and machine learning," *IEEE Transactions on Signal Processing*, vol. 65, no. 3, pp. 794–816, 2017.